

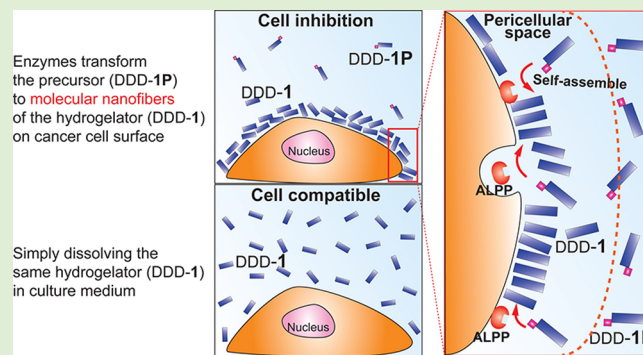
D-Amino Acids Modulate the Cellular Response of Enzymatic-Instructed Supramolecular Nanofibers of Small Peptides

Junfeng Shi, Xuewen Du, Dan Yuan, Jie Zhou, Ning Zhou, Yibing Huang,[†] and Bing Xu*

Department of Chemistry, Brandeis University, 415 South Street, MS 015, Waltham, Massachusetts 02453, United States

S Supporting Information

ABSTRACT: Peptides made of D-amino acids, as the enantiomer of corresponding L-peptides, are able to resist proteolysis. It is, however, unclear or much less explored whether or how D-amino acids affect the cellular response of supramolecular nanofibers formed by enzyme-triggered self-assembly of D-peptides. In this work, we choose a cell compatible molecule, Nap-L-Phe-L-Phe-L_PTyr (LLL-1P), and systematically replace the L-amino acids in this tripeptidic precursor or its hydrogelator by the corresponding D-amino acid(s). The replacement of even one D-amino acid in this tripeptidic precursor increases its proteolytic resistance. The results of static light scattering and TEM images show the formation of nanostructures upon the addition of alkaline phosphatase, even at concentrations below the minimum gelation concentration (mgc). All these isomers are able to form ordered nanostructures and exhibit different morphologies. According to the cell viability assay on these stereochemical isomers, cells exhibit drastically different responses to the enantiomeric precursors, but almost same responses to the enantiomeric hydrogelators. Furthermore, the different cellular responses of LLL-1P and DDD-1P largely originate from the ecto-phosphatases catalyzed self-assembly of DDD-1 on the surface of cells. Therefore, this report not only illustrates a new way for tailoring the properties of supramolecular assemblies, but also provides new insights to answering the fundamental question of how mammalian cells respond to enzymatic formation of nanoscale supramolecular assemblies (e.g., nanofibers) of D-peptides.



INTRODUCTION

This article reports that the incorporation of D-amino acids into small peptides not only changes the stereochemistry of the molecules, but also modulates the biological activities (e.g., cytotoxicity) of the supramolecular assemblies^{1–3} (e.g., nanofibers) of the small peptides formed by enzyme-instructed molecular self-assembly. Being the enantiomers of L-amino acids, D-amino acids rarely serve as the building blocks of naturally occurring proteins. This feature allows D-peptides to resist proteolysis catalyzed by endogenous proteases *in vivo*. Such a relatively long-term biostability has stimulated the exploration of a variety of biological or biomedical applications of D-amino acids. For example, D-amino acids have served as building blocks of D-peptides for tracing the lineage of cells⁴ and the growth of axons,⁵ disrupting protein interactions,^{6–8} preventing HIV-1 entry,^{9–11} blocking mechanosensitive channels,¹² decreasing the freezing point,¹³ targeting DNA,¹⁴ reducing adverse drug reactions (ADR) of anti-inflammatory drugs,¹⁵ and inhibiting the aggregation of β -amyloid ($A\beta$).¹⁶ The integration of D-amino acids with other molecular motifs has resulted in bacterial peptidoglycan,¹⁷ antimicrobial agents,^{18–20} and natural products.²¹ More importantly, the combination of D-amino acids with L-amino acids to form peptides or proteins offers new and rich structures or functions^{22–24} that are otherwise difficult to access, such as

conformation control of cyclic-RGD²⁵ for binding integrin, destabilization of peptide helices,²⁶ sustaining drug or dye delivery via participation to the supramolecular structure,^{27,28} triggering three-stranded β -sheet to form β -sheet-rich fibrils,²⁹ and constraining hydrogen bonding of linear peptides in water.³⁰ These advantages have also stimulated the recent successful development of *in vitro* translation of D-amino acids into proteins via charging tRNA with D-peptides.^{31,32}

Besides expanding the stereochemical space of molecules, the use of D-amino acids has led to novel supramolecular structures. For example, the elegant design of D,L-peptides allows the formation of nanotubes,³³ as well as nanoribbons, nanotapes, twisted fibers, and bundles,^{24,28,34,35} the incorporation of a D-proline establishes β -hairpin for a novel class of peptide hydrogels,³⁶ and the coassembly of D-peptides with L-peptides has generated rippled β -sheet.³⁷ Encouraged by these results, we have been using D-amino acids for developing supramolecular nanofibers/hydrogels.^{15,35,38–43} Our previous works show that the integration of D-amino acid with D-glucosamine afford a supramolecular hydrogel for wound healing,⁴² the hydrogels made from D-amino acids are suitable for sustained

Received: June 2, 2014

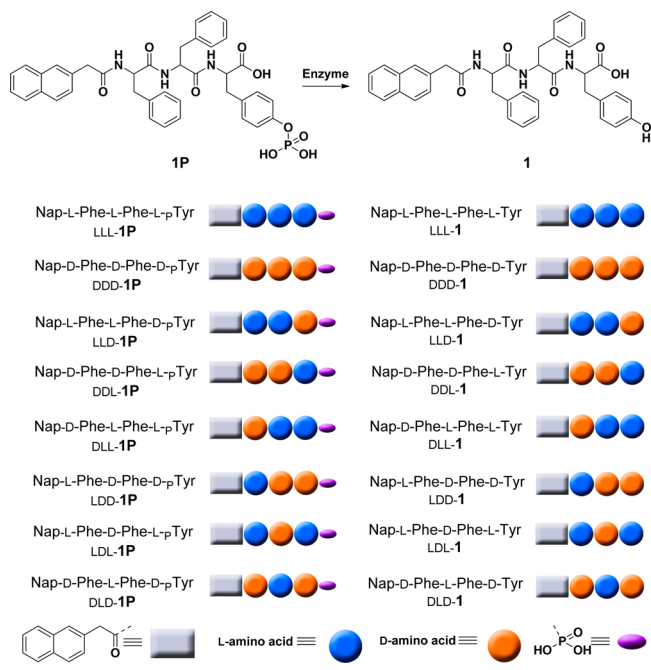
Revised: September 2, 2014

Published: September 5, 2014

drug release *in vivo*,⁴⁰ and the incorporation of D-amino acid residues in small peptide hydrogelators enhances their resistance to proteolysis.^{39,43} Moreover, our recent studies show that, not only do the D-peptides boost the selectivity of a nonsteroidal anti-inflammatory drug (NSAIDs),¹⁵ but also certain D-peptides (e.g., peptides containing D-tyrosine phosphate) can serve as the substrates of appropriate endogenous enzymes (e.g., phosphatases), without affecting the rate of dephosphorylation.³⁸ While these advances by our group as well as others^{27,44,45} highlight the promises of the use of D-amino acid-based materials for potential biomedical applications, they also underscore the importance of evaluating the cellular responses to the self-assembly of small peptides containing D-amino acids, which has just begun to be explored systematically.

To evaluate how the D-amino acids modulate the biological activities of supramolecular nanofibers^{46–49} formed by enzyme-instructed self-assembly,^{50–58} we systematically replaced the L-amino acids in a tripeptidic hydrogelator⁵⁹ (LLL-1) or its precursor⁶⁰ (LLL-1P) by D-amino acids and examined the viability of mammalian cells incubated with the stereochemical isomers of the precursors and the hydrogelators. Our results show that all of these isomers (Scheme 1) are able to form

Scheme 1. Molecular Structures of the Precursors and the Corresponding Hydrogelators that are Enantiomeric Isomers



supramolecular hydrogels when alkaline phosphatase catalyzes the dephosphorylation of the precursors to result in the hydrogelators. As expected, the molecules of different isomers self-assemble in water to form nanofibers that exhibit different morphologies. The use of proteinase K, a powerful endopeptidase, to treat the precursors reveals that the incorporation of even one D-amino acid in this tripeptidic precursor decreases the proteolysis catalyzed by proteinase K and the incorporation of D-amino acid residues in the middle position of the tripeptidic backbone also enhances the proteolytic resistance of the hydrogelators. Static light scattering and TEM images reveal the formation of nanofibers

upon the addition of alkaline phosphatase, even at concentrations (e.g., 200 μ M) below the minimum gelation concentrations (mgc; e.g., DDD-1: 1.0 mM). Unexpectedly, while most of the enantiomer pairs of the hydrogelators lead to almost the same cellular responses, the enantiomer pairs of the precursors result in different cellular responses. For example, while the precursor LLL-1P exhibits little inhibition on cell proliferation at a concentration as high as 500 μ M, the IC₅₀ of its enantiomer (precursor DDD-1P) is about 279 μ M against HeLa cells. In contrast, both enantiomers of the hydrogelators (e.g., LLL-1 and DDD-1) appear to be cell compatible even at 500 μ M. These results indicate that these stereochemical isomers exhibit quite different biological properties due to the introduction of D-amino acids and the enzyme-triggered self-assembly. These results contribute new insights to answering the fundamental question on how mammalian cells respond to D-amino acids or D-peptides (e.g., containing aromatic group(s)) as the self-assembly promoter^{40,42,60,61} when the self-assembly of the D-peptides integrates with endogenous enzymatic reactions. In addition, these results indicate that judicious incorporation of D-amino acid(s) into peptidic hydrogelators (and their precursors) is a feasible and useful method to modulate the morphological and biological properties of supramolecular assemblies of small peptides.^{48,50,62–66} The fundamental conceptual advance of this work is that ecto-phosphatases (e.g., placental alkaline phosphatases) have spatiotemporal control over the formation of the nanofibers of the small peptides, thus inhibiting cancer cells.⁸⁶

MATERIALS AND METHODS

A. Materials. Alkaline phosphatase (ALP) was purchased from Biomatik USA, 2-naphthylacetic acid from Alfa Aesar, N,N-diisopropylethylamine (DIPEA), and O-benzotriazole-N,N,N',N'-tetramethyl-uronium-hexafluoro-phosphate (HBTU) from Acros Organics USA, all amino acid derivatives from GL Biochem (Shanghai) Ltd.

B. Instrument. LC-MS on Waters Acquity ultra Performance LC with Waters MICROMASS detector, rheological measurement on ARES-G2 rheometer; electron microscopy was performed on a FEI Morgagni 268 TEM with a 1k CCD camera (GATAN, Inc., Pleasanton, CA); MTT assay for cell toxicity test on DTX880 Multimode Detector.

C. Peptide Synthesis and Purification. According to the structures shown in Scheme 1, we synthesized the precursors and the hydrogelators using conventional SPPS.⁶⁷ The procedure reported by Alewood⁶⁸ gives tyrosine phosphate in 90% yield. Following an established procedure,⁶⁹ it is easy to obtain Fmoc-protected tyrosine phosphate for further reaction, which starts with loading Fmoc-p-Tyr-OH (or Fmoc-Tyr-OH for synthesis of hydrogelators) at the C-terminal onto 2-chlorotriptyl chloride resin for SPPS.⁶⁷ The removal of the protecting group by 20% piperidine allows the coupling of Fmoc-Phe-OH to the free amine group by using N,N-diisopropylethylamine/O-benzotriazole-N,N,N',N'-tetramethyl-uronium-hexafluoro-phosphate (DIPEA/HBTU) as the coupling agent. At the final step, 2-naphthylene acetic acid reacts to the N-terminal tripeptide. The resin-bound peptide was cleaved using a cocktail of TFA/triisopropylsilane/water (95:2.5:2.5) for 2 h under nitrogen, then collecting the filtrate, and washing the resin twice using TFA. Crude product was obtained after the addition of cold diethyl ether into concentrated filtrate. The crude product was purified by reverse phase high performance liquid chromatography (HPLC) using a semiprepare C18 column. HPLC solvents consisted of solvent A (0.1% TFA in water) and solvent B (0.1% TFA in acetonitrile). The precursors were purified by linear gradient of 20–60% B in 22 min, the desired compound eluted at 17 min. The resulting peptide solution was frozen by liquid nitrogen and lyophilized to afford purified precursors in fair yields (40–60%). A

similar SPPS procedure affords the corresponding hydrogelators in around 80% yields after purification.

D. General Procedure for Hydrogel Preparation. All precursors (2.4 mg) were dissolved in 400 μ L of PBS buffer (pH 7.4), the hydrogels formed after the addition of ALP (12.5 U/mL). The samples were aged for 2 days before measurement;⁷⁰ we choose to age the gels to allow adequate time for completely converting the precursors into hydrogelators.

E. Circular Dichroism Measurement (CD). CD spectra were recorded (180–350 nm) using a JASCO 810 spectrometer under a nitrogen atmosphere. The hydrogel (0.6%, 200 μ L) was placed evenly on the 1 mm thick quartz cuvette and scanned with 0.5 nm interval three times. The CD spectra in Figure S9 confirm the chirality of enantiomeric pairs of the peptides.

F. Rheological Measurement. Rheological tests were conducted on TA ARES-G2 rheometer, parallel-plate geometry with an upper plate diameter of 25 mm was used during the experiment, and the gap was 0.4 mm. During the measurement, the stage temperature was maintained at 25 °C by Peltier heating cooling system. The hydrogel was loaded into stage by spatula, and then we performed dynamic strain (0.1–100%) at 6.28 rad/s, the strain for maximum G' in the linear range of strain sweep test was picked for frequency sweep test (0.1–200 rad/s).

G. TEM Measurement. Aliquots (3–5 μ L) of sample solutions were added into glow discharge thin carbon-coated copper grids (400 meshes, Pacific Grid-Tech) and incubated for 30 s at room temperature. Excess sample solution was removed by blotting with filter paper touched to the edge of the grid. After removing excess fluid, the grid was washed with three successive drops of deionized water and then exposed to three successive drop 2.0% (w/v) uranyl acetate. Data were collected at high vacuum on Morgagni 268 transmission electron microscope.

H. Dephosphorylation Assay. Typically, 4 mL of precursor solution in PBS buffer (500 μ M, pH = 7.4) was treated with ALP (0.1 U/mL) at 37 °C. A total of 100 μ L of sample was taken out at the desired time and mixed with 100 μ L of methanol. The obtained samples were analyzed by analytic HPLC to determine the amount of precursor and hydrogelator.

I. MTT Assays. We seeded 2×10^4 (cells/well)⁷¹ of HeLa cells into a 96-well plate (Obtained from Falcon) with 100 μ L of MEM medium supplemented with 10% fetal bovine serum (FBS), 100 U/mL penicillin, and 100 μ g/mL streptomycin. Incubation at 37 °C and 5% CO₂ for 12 h allowed HeLa cells to attach to the bottom of the 96-well plate. Then we replaced the medium with another 100 μ L of growth medium that contained serial diluents of our compounds and then incubated the cells at 37 °C and 5% CO₂ for an additional 72 h. During the viability measurement of HeLa cells, which were assayed for 3 days, we added 10 μ L of (3-(4,5-dimethylthiazol-2-yl)-2,5-diphenyl-tetrazolium bromide (MTT, 0.5 mg/mL) into the assigned wells in their corresponding day every 24 h, which was followed by adding 100 μ L of 0.1% sodium dodecyl sulfate (SDS) 4 h later. We then collected the assay results after 24 h incubation. Since the mitochondrial reductase in living cells reduced MTT to purple formazan, the absorbance at 595 nm of the whole solution was finally measured by DTX 880 Multimode Detector. With MEM medium as blank and untreated HeLa cells as control, we measured each concentration of these compounds in triplicate. The IC₅₀ values of our hydrogelators were read from their activity curves on day 2.

J. General Procedure for Digestion Experiment. A total of 3 mL of solution of different compounds in HEPES buffer (10 mM, pH = 7.5) were treated with proteinase K (3.0 U/mL) at 37 °C. A 100 μ L aliquot of sample was taken out at the desired time and mixed with 100 μ L of methanol. The obtained samples were analyzed by HPLC to determine the amount of compound remaining in solution.

K. Identification and Quantification of Residue Compounds in Culture Medium. A total of 4.0×10^6 of cells in exponential growth phase were seeded into 10 mL Petri dish with 10 mL culture medium. After 4 h attachment, we replaced the medium with another 10 mL culture medium containing precursors at 300 μ M and then

incubated the cells at 37 °C and 5% CO₂ for 24 h. The culture medium was collected and diluted with methanol for LC-MS analysis.

L. Light Scattering Measurement. The static light scattering experiments were performed using an ALV (Langen, Germany) goniometer and correlator system with a 22 mW HeNe (λ = 633 nm) laser and an avalanche photodiode detector. All samples were filtered by using 0.22 μ m filters. The addition of ALP (0.5 U/mL) to the solution of precursors for 24 h, we obtained corresponding samples of hydrogelators. The SLS tests were carried out at room temperature, and the angles of light scattering we chose were 30, 60, 90, and 120°, respectively. The resulting intensity ratios are proportional to the amount of aggregates in the samples.

RESULTS AND DISCUSSION

Molecular Design. In our recent work, we found that a dipeptide derivative, Nap-L-Phe-L-Phe (NapFF),^{40,72} not only exhibits remarkable ability to self-assemble in water to form supramolecular nanofibers and a hydrogel, but also, after being taken into cells, disrupts the dynamics of microtubules and induces the apoptosis of glioblastoma cells. More importantly, the nanofibers of NapFF are innocuous to model neuron cells (e.g., PC-12).^{73,77} This result suggests that it is possible to use the nanofibers of small molecules to target cancer cells selectively. Since some more metastatic cancer cells overexpress phosphatase,⁷⁴ we chose to attach a phosphatase substrate, tyrosine phosphate (L_pTyr), to a self-assembly motif (e.g., NapFF⁷²) for generating nanofibers upon the action of phosphatases from cancer cells as a way to inhibit cancer cells. Thus, we decided to examine the precursor Nap-L-Phe-L-Phe-L_pTyr (LLL-1P), which is an easily accessible tripeptide derivative known to form nanofibers upon the treatment of phosphatase (e.g., ALP).⁶⁰ Because our previous studies prove that peptides containing D-tyrosine phosphate (D_pTyr) are able to act as the substrates of phosphatase without reducing the rate of dephosphorylation,^{15,38,41} we also chose D_pTyr to connect with NapFF. This choice leads to the question about the role of D-amino acid in the nanofibers of the tripeptidic derivatives. To investigate how D-amino acids affect the biological activity of supramolecular nanofibers formed by enzyme-triggered self-assembly of the tripeptides, we used D-Phe,^{75,76} and D-Tyr to replace the corresponding L-amino acid(s) in the precursor LLL-1P (or hydrogelator LLL-1). Such a systematic design requires the synthesis of eight precursors and eight hydrogelators (Scheme 1). Among them, there are four enantiomer pairs in either the precursors or their corresponding hydrogelators.

Enzyme-Triggered Self-Assembly and Hydrogelation.

To evaluate the effects of D-amino acids on the enzymatic hydrogelation process, we treated the solutions of the precursors with alkaline phosphatase (ALP) and examined the resulting hydrogels. As shown in the insets of Figure 1, the addition of ALP (12.5 U/mL) to the solutions of the stereochemical isomers of 1P (0.6 wt % in PBS buffer) converts the precursors to the corresponding hydrogelators of 1. All the hydrogelators resulted in hydrogels, except the hydrogel of DLD-1, which is relatively weak. For example, LLL-1 and DDD-1 are able to form transparent hydrogels that support their own weights and are stable for more than six months. Like the hydrogels of LLL-1 and DDD-1, the hydrogels of LLD-1 and DLL-1 are transparent, but they exhibit slight syneresis and shrink a little after several weeks. Both the solutions of DLL-1P and LDD-1P turn into stable hydrogels after the treatment of ALP. While the hydrogels of DLL-1 and LDD-1 recover quickly after shearing, the hydrogel

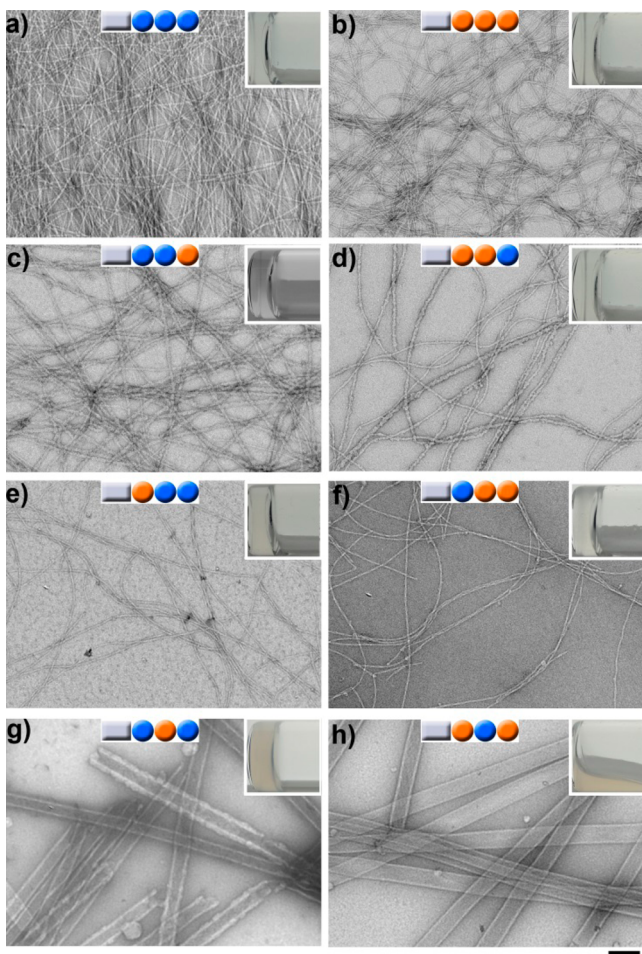


Figure 1. TEM images of the hydrogels (inset: optical images) of (a) LLL-1, (b) DDD-1, (c) LLD-1, (d) DDL-1, (e) DLL-1, (f) LDD-1 (g), LDL-1, and (h) DLD-1, formed by the addition of alkaline phosphatase (12.5 U/mL) to the solution of their corresponding precursors (LLL-1P, DDD-1P, LLD-1P, DDL-1P, DLL-1P, LDD-1P, LDL-1P, and DLD-1P) at the concentration of 0.6 wt % in PBS buffer (scale bar = 100 nm).

of LDL-1 fails to restore quickly to gel state after being disrupted mechanically (by spatula). Interestingly, at the same concentration, DLD-1 forms a slightly weaker hydrogel than the hydrogel formed by LDL-1, which is consistent with their small storage moduli and critical strain for LDL-1 (0.0067 Pa, 2.5%) and DLD-1 (0.022 Pa, 0.9%). These results, though indicating the subtle effects of the position of the D-amino acids in these tripeptidic derivatives, confirm that the peptide containing D-tyrosine phosphate can serve as the substrate of alkaline phosphatase (ALP).³⁸

Rheometry. We used rheometry to compare the hydrogels made by the stereochemical isomers shown in Scheme 1. As shown in Table 1, the values of storage moduli are always larger than those of loss moduli (Figure S2), indicating that all samples (including the hydrogel of DLD-1) behave as solid-like materials. Additionally, the modulus-strain profile provides the maximum modulus G_0 in the linear range and the value of critical strain (Y_0) at which the value G' starts to decrease sharply due to the loss of cross-linking within the gel network.⁷⁸ The hydrogel of LLL-1 has G_0 of 0.28 KPa and Y_0 of 3.0%, agreeing with our previous report that LLL-1 is able to form a stable hydrogel.⁷⁶ The hydrogel of DDD-1 has the largest value

Table 1. Summary of the Properties of Self-Assemblies of the Precursors and Their Corresponding Hydrogels

comp.	LLL-1P	DDD-1P	LLD-1P	DLL-1P	LDD-1P	LDL-1P	DLD-1P
+ ALP	gel	gel	gel	gel	gel	gel	gel ^a
G_0^b (KPa)	0.28	0.097	1.1	1.8	0.93	1.1	0.022
Y_0^c (%)	3.0	4.0	3.0	2.3	2.7	2.1	0.90
G'^{d} (KPa)	0.27	0.09	1.4	1.8	1.0	1.1	0.026
G''^{d} (KPa)	0.064	0.01	0.33	0.42	0.20	0.20	0.0076
morphology of the network in the gel (width, nm)	fibers (8 ± 2)	fibers (8 ± 2, 13–25 ± 2)	fibers (8 ± 2, 25–50 ± 2)	helical fibers ^e (12 ± 2)	helical fibers ^f (10 ± 2)	tubes (35–70)	tubes (55–70)
$I\!C_{50}$ of IP (μM)	>500	279	428	335	>500	500	>500
$I\!C_{50}$ of 1 (μM)	>500	>500	412	400	401	400	287
proteolytic products of 1P ^g	L-2	DDD-1P	LLD-1P	DLL-1P	DLL-2 ^h	LLD-1P	DLD-1 ⁱ
proteolytic products of 1	L-2	DDD-1	LLD-1	DLL-1	LLD-1	LLD-1	DLD-1 ⁱ
morphology of IP at 500 μM	fibers (8 ± 2)	fibers (8 ± 2)	fibers (8 ± 2)	fibers (8 ± 2)	fibers (9 ± 2)	fibers (9 ± 2)	nonfibrillar

^aDLD-1 forms a weak gel. ^bThe maximum modulus in the linear range of strain sweep profile. ^cThe critical strain. ^dThe modulus at the frequency of 10 rad/s. ^eHelical pitch = 50 nm. ^fHelical pitch = 45 nm. ^gThe compounds remaining after treatment with proteinase K for precursors 1P and hydrogels 1. ^hDLL-2 indicates Nap-D-Phe-L-Phe. 88% DLD-1 and 12% Nap-D-Phe-L-Phe.

of critical strain (4.0%) among all the hydrogels, while its G_0 is 0.097 kPa. Due to the heterogeneity of the hydrogels, the G' of the hydrogel of LLL-1 is larger than that of the hydrogel of DDD-1, which agrees with observation of their TEM (Figure 1a,b). Furthermore, since the presence of the enzyme in the hydrogels, the enzymatically formed hydrogels of DDD-1 and LLL-1 are diastereomeric systems; thus, it is reasonable to observe a rheological difference between them. The hydrogels of LLD-1 and DDL-1 have close values of G_0 , 1.1 kPa (LLD-1) and 1.8 kPa (DDL-1), as well as close values of Y_0 (3.0% for LLD-1 and 2.3% for DDL-1). The storage moduli of the hydrogels of LLD-1 and DDL-1 increase around 4–5-fold compared to that of the hydrogel of LLL-1, indicating that the replacement of the L-amino acid (or D-amino acid) by corresponding D-amino acid (or L-amino acid) could change the rheological properties of the hydrogels. The values of G_0 of the hydrogels of DLL-1 and LDD-1 are 0.93 and 1.1 kPa, respectively, and the corresponding values of critical strain (Y_0) are 2.7 and 2.1%. In contrast, after changing the position of D-phenylalanine in the tripeptide of DLL-1P and LDD-1P, the resulting hydrogel of LDL-1 has the lowest G_0 (6.8 Pa), while gel DLD-1 has the lowest values of critical strain (0.9%). This implies that the position of D-amino acid also could affect the rheological properties of the hydrogels. These results also indicate that the hydrogels of the enantiomer pairs exhibit similar viscoelastic properties and the incorporation of D-amino acid likely modulates the elasticity of the hydrogels via forming different supramolecular structures, as confirmed by TEM (vide infra) and observed in previous self-assembled tripeptide hydrogels.^{24,75,76,79}

TEM of the Hydrogels. We used TEM to examine the nanoscale morphologies of the matrices of the hydrogels. As shown in Figure 1a, the TEM images in the hydrogel of LLL-1 shows long, flexible nanofibers with diameters of 8 ± 2 nm. Similarly, the hydrogel of DDD-1 (Figure 1b) also consists of nanofibers with width around 8 nm. In both case, the nanofibers tend to form a considerable amount of bundles, reflecting the significant interfiber interactions. TEM image in the hydrogel of LLD-1 (Figure 1c) reveals two kinds of morphologies: large nanofibers and slim nanofibers. The slim nanofibers have lengths around several micrometers and diameter of 8 ± 2 nm; the width of large nanofibers ranges from 13 to 20 nm. Like LLD-1, hydrogel of DDL-1 (Figure 1d) also contains large nanofibers and slim nanofibers. The slim nanofibers have similar width (around 8 nm) with that in the hydrogel of LLD-1. The width of large nanofibers, ranging from 25 to 50 nm, is almost twice of that of the hydrogel of LLD-1. These large nanofibers, which consist of the slim nanofibers, likely contribute to the relatively large storage moduli of the hydrogels of LLD-1 and DDL-1. In Figure 1e, TEM image of the hydrogel of DLL-1 shows individual nanofibers and helical nanofibers. The individual nanofibers have width 6 ± 2 nm. Apparently, two single nanofibers twist each other to form helical nanofibers with a diameter of 12 nm and a helical pitch of around 50 nm (Figure S3A). Similarly, the hydrogel of LDD-1 (Figure 1f) contains twisted nanofibers with width of 10 nm and helical pitch of 45 nm (Figure S3B). The enantiomer pair of LDL-1 and DLD-1 self-assemble to form similar nanotubes with widths ranging from 46 to 70 nm (Figure 1g and 1h). These nanotubes form poorly cross-linked networks, which explain the weak stability of gel LDL-1 and DLD-1. The morphology of the nanofibers of LDL-1 (or DLD-1) differs significantly from those of the other three pairs of enantiomeric

hydrogelators, likely originating from the alternation of D-amino acid and L-amino acid residues in the tripeptides because such alternation results in the side-chain of the amino acids on the same side of the peptides. These results suggest that incorporation of D-amino acid is able to modulate the morphologies of the matrices of supramolecular hydrogels. The different morphologies are not only responsible for the difference in the rheological properties of the supramolecular hydrogels, but also imply that the position of D-amino acids in the tripeptides likely affects the self-assembly of the hydrogelators.

Cell Viability. To investigate how D-amino acids affect the cellular response to the tripeptidic precursors and hydrogelators, we used MTT (3-(4,5-dimethylthiazol-2-yl)-2,5-diphenyl tetrazolium bromide) assay to examine cell viability of the HeLa cells incubated with the stereochemical isomers shown in Scheme 1. One unique feature of the results of the cell viability test is that the cytotoxicities of the precursors or hydrogelators usually deviate from the sigmoidal dose response law.⁸⁰ Thus, we define the calculated concentration of 50% inhibition from these experiments as “apparent IC₅₀”, though it is denoted as IC₅₀. As shown in Figure 2, the IC₅₀ values of the

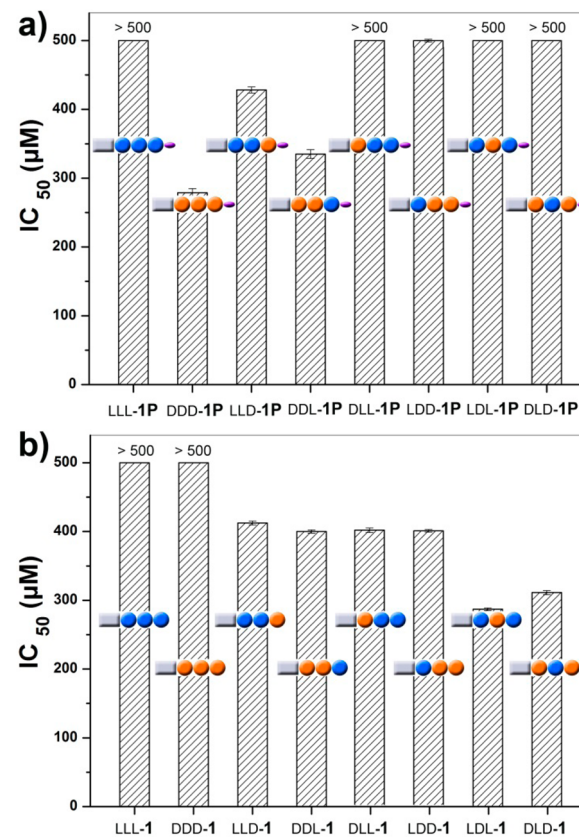


Figure 2. IC₅₀ values of (a) the precursors and (b) the hydrogelators against HeLa cells at 48 h.

precursors LLL-1P and DDD-1P are >500 and 279 μM, respectively. Although this result apparently suggests that the incorporation of D-amino acids increases the cytotoxicity, the corresponding hydrogelators of LLL-1 and DDD-1, which are the products of the enzyme-catalyzed dephosphorylation of the precursors LLL-1P and DDD-1P, hardly inhibit cell proliferation even at 500 μM. Similar to the case of LLL-1P and DDD-1P, while the values of IC₅₀ of LLD-1P and DDL-1P are

different, 428 and 335 μM , respectively, their corresponding hydrogelators exhibit similar values of IC_{50} , 412 μM for LLD-1 and 400 μM for DDL-1. Like LLL-1P and DDD-1P, the enantiomer pair, DLL-1P and LDD-1P, inhibits cell proliferation differently. That is, at 500 μM , DLL-1P is cell compatible, but LDD-1P inhibits around 50% of cells. Their corresponding hydrogelators DLL-1 and LDD-1, again, show similar cytotoxicity: the values of IC_{50} are 401 μM (DLL-1) and 400 μM (LDD-1), respectively. While the enantiomer pair, LDL-1P and DLD-1P, are cell compatible (IC_{50} values $>500 \mu\text{M}$), their corresponding hydrogelators, LDL-1 and DLD-1, also show close cytotoxicity, the values of IC_{50} (287 μM for LDL-1 and 311 μM for DLD-1). Obviously, these results indicate that enantiomeric precursors exhibit dramatically different cellular responses, while enantiomeric hydrogelators show similar cytotoxicities. Particularly, the precursors with more D-amino acid substitution are more toxic than their corresponding enantiomers (except enantiomeric pair LDL-1P and DLD-1P). Such differences are clearly associated with enzyme-instructed self-assembly, which exclude that the cytotoxicity is due to the amphiphilic precursors behaving as surfactants.

Biostability. To understand the results from the cell viability assay (Figure 2) and to investigate the influence of the D-amino acid(s) on the proteolytic stability of the precursors, we used a powerful endopeptidase, proteinase K, to treat these precursors at a concentration of 500 μM . As revealed in Figure 3a, all precursors, except LLL-1P, exhibit

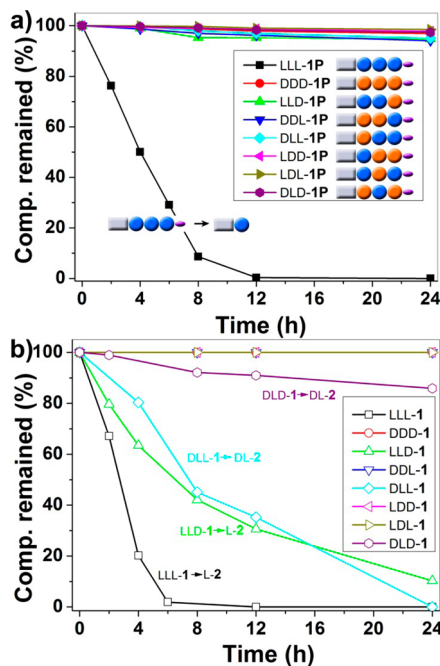


Figure 3. Digestion curve of precursors (a) and hydrogelators (b) upon treatment with proteinase K (3 U/mL) for 24 h. All compounds are at the concentration of 500 μM ; L-2 and DL-2 indicates Nap-L-Phe and Nap-D-Phe-L-Phe, respectively.

excellent resistance toward proteolytic digestion. This result indicates that the incorporation of even one D-amino acid in this tripeptide precursor is able to reduce proteolytic hydrolysis of the precursors. LC-MS indicates that LLL-1P proteolytically hydrolyzes to L-2 upon treatment with proteinase K for 12 h, suggesting that the phosphate group on the tripeptide, alone, is unable to prevent the digestion by proteinase K. Since L-2 is

innocuous to cells even at 500 μM , the proteolysis of LLL-1P likely contributes to its cell compatibility. In contrast, DDD-1P hardly undergoes proteolysis in the presence of proteinase K. As shown in Figure 3a, more than 94% of LLD-1P, DDL-1P, DLL-1P, LDD-1P, LDL-1P, and DLD-1P remain upon treatment with proteinase K for 24 h. These results indicate that the incorporation of one D-amino acid to the tripeptidic precursors, regardless of position, renders the precursors to have proteolytic resistance.

Interestingly, unlike their corresponding precursors, the hydrogelators exhibit quite different proteolytic stability in the presence of proteinase K. As shown in Figure 3b, the hydrogelators having D-amino acid residues in the middle position of the tripeptides (e.g., DDD-1, DDL-1, LDD-1, and LDL-1) exhibit excellent proteolytic resistance. That is, almost 100% of those tripeptide derivatives remain after incubation with proteinase K for 24 h. However, the hydrogelators having L-amino acid residues in the middle position of the tripeptides (e.g., LLL-1, LLD-1, DLL-1, and DLD-1) undergo, albeit at different rates, proteolysis in the presence of proteinase K. The rate of proteolysis decreases in the order of LLL-1, LLD-1, DLL-1, and DLD-1 which appears to agree with the trend of the IC_{50} values of these four hydrogelators. The proteolytic resistant hydrogelators, however, exhibit the same trend of the decrease of IC_{50} values as that of proteolytic susceptible hydrogelators. These results indicate that the IC_{50} values of the tripeptidic hydrogelators unlikely correlate with their proteolytic susceptibilities only. Particularly, although these results suggest that the difference in proteolytic resistance likely contributes to the different cellular responses to LLL-1P and DDD-1P, it is unable to explain the same cell compatibility of LLL-1 and DDD-1.

Due to the existence of many endopeptidases in cells,⁸¹ it is necessary to know the stability of the precursors in a cellular environment to establish the spatiotemporal profiles of the tripeptidic derivatives and their assemblies. Thus, we used HeLa cell to incubate with precursors (300 μM) at 37 °C for 24 h and then collected culture medium for LC-MS analysis. As shown in Figure 4, except for LLL-1P (which became L-2), all the residue compounds in the culture medium are their corresponding hydrogelators. This result is not only consistent with the digestion curve in Figure 3a, but also confirms that the

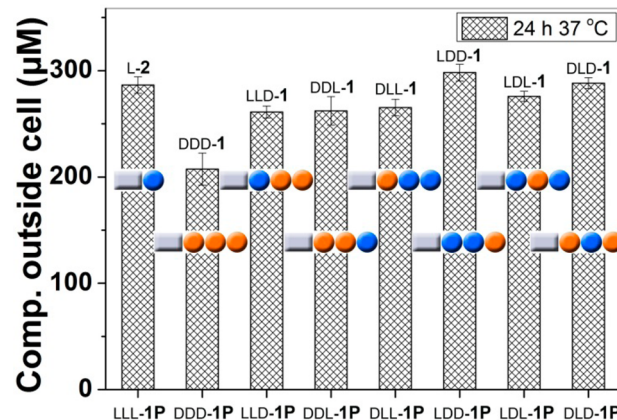


Figure 4. Concentrations of residue compounds in the culture medium after incubation of HeLa cells with precursors (300 μM) at 37 °C for 24 h. LC-MS was used to identify and quantify the residue compounds in culture medium.

endogenous phosphatases from HeLa cells,⁷⁴ indeed, catalyze the dephosphorylation of the precursors within 24 h. The results in Figure 4 also agree with the enhanced biostability of tripeptidic precursors after incorporation of D-amino acid(s), even *in vivo*.⁴⁰

Dephosphorylation. One possibility is that DDD-1P and LLL-1P have different rates of dephosphorylation, which results in different cytotoxicities. To evaluate the effect of D-amino acid(s) on the rate of dephosphorylation of the precursors, we used ALP (0.1 U/mL) to treat the precursor at 500 μM. As shown in Figure 5, the rate of dephosphorylation of DDD-1P is

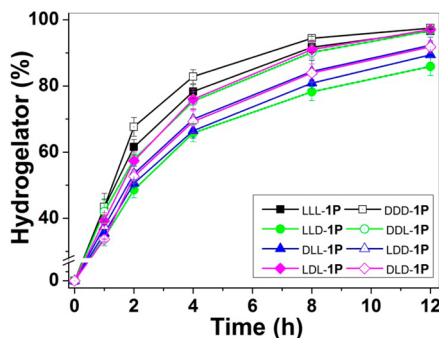


Figure 5. Increase of hydrogelators with time shows the dephosphorylation process of the precursors after incubation with ALP (0.1 U/mL) at 37 °C. The precursors dissolve in pH 7.4 PBS buffer at a concentration of 500 μM.

comparable (appearing slightly faster at the initial stage) to that of LLL-1P under the same conditions. This result is consistent with our previous study that shows ALP will dephosphorylate D-tyrosine phosphate and L-tyrosine phosphate at almost the same rate.³⁸ Like LLL-1P and DDD-1P, enantiomer pair LDD-1P and DLL-1P also shows similar dephosphorylation rates. About 90% LDD-1P and DLL-1P convert to their corresponding hydrogelators after being incubated with ALP for 12 h. In the case of DDL-1P/LLD-1P and LDL-1P/DLD-1P, the rates of the dephosphorylation of DDL-1P and LDL-1P are higher than those of their corresponding enantiomers (i.e., LLD-1P and DLD-1P). Except the enantiomeric pair of LDL-1P/DLD-1P, the precursors with higher rates of dephosphorylation exhibit higher cytotoxicity than their enantiomers. This result suggests that the difference in enzymatic dephosphorylation rate contributes to the difference in the rate of nanofiber formation, thus, resulting in different cellular responses of enantiomeric precursors.

Interestingly, the concentration of DDD-1 (208 μM) in the culture medium is the lowest among all the hydrogelators formed by the dephosphorylation of the precursors (Figure 4). Despite its proteolytic susceptibility, as the enantiomer of DDD-1, the concentration of LLL-1 in the culture medium is 287 μM. Such a discrepancy suggests that a significant amount of DDD-1 molecules are present either inside cells or on the cell surface (i.e., in the pericellular space of HeLa cells). Indeed, the DDD-1P at 300 μM could form hydrogel on HeLa cells after 24 h incubation at 37 °C (as shown in Figure S11). Since it is known that the overexpression of placental alkaline phosphatase (ALPP, as an ecto-phosphatase) on the surface of HeLa cell,^{82–84} we used L-phenylalanine to inhibit ALPP during cell culture.⁸⁵ As shown in Figure 6a, the cytotoxicity of DDD-1P against HeLa cell decreases after the addition of certain amount L-phenylalanine (e.g., 0.3 mM and 1.0 mM). Since L-

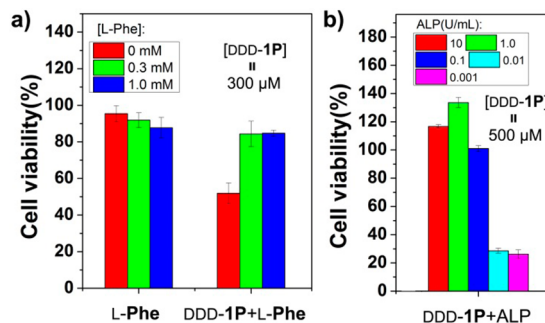


Figure 6. (a) Viability of HeLa cell incubated with L-Phe and (L-Phe + DDD-1P) for 48 h; (b) Cytotoxicity of DDD-1P after addition of different amounts of ALP after 48 h.

phenylalanine is cell compatible below the concentration of 1.0 mM, the reduced cytotoxicity of DDD-1P is likely due to the inhibition of ALPP by L-phenylalanine.⁸⁵ This result suggests that ecto-phosphatases likely catalyze the formation of DDD-1 and its self-assembly on cell surface for inhibiting the growth of HeLa cells, indicating that the spatiotemporal control of the self-assembly of DDD-1 is a critical factor for determining the cytotoxicity of DDD-1P and DDD-1.

To further confirm the critical role of endogenous ecto-phosphatases, we added ALP (at 10, 1.0, 0.1, 0.01, or 0.001 U/mL), as an exogenous enzyme, to DDD-1P instantly before treating the HeLa cells. As shown in Figure 6b, the addition of exogenous ALP (at 0.1 U/mL or above) completely abrogates the cytotoxicity of DDD-1P. This result therefore proves that endogenous enzymatic dephosphorylation is critical for the cellular response to DDD-1P. Our recent study confirms that the dephosphorylation of DDD-1P by the endogenous phosphatases on the cell surface, indeed, causes the self-assembly of DDD-1 on the cell surface to form a hydrogel in the pericellular space. Meanwhile, the incubation of HeLa cell with DDD-1 at 560 μM fail to form pericellular hydrogel since it distributed evenly in the cell culture medium.⁸⁶ This result also explains why DDD-1P and DDD-1 exhibit quite different cellular responses. The concentrations of other hydrogelators in culture medium are at least 260 μM, suggesting that the positions and the numbers of the D-amino acids also affect distribution of the hydrogelators in cellular environment.

Static Light Scattering and TEM below mgc. To understand the different cell viabilities exhibited by non-enantiomeric precursors and hydrogelators, we examined their self-assembly below mgc. To evaluate the self-assembly of the hydrogelators (or the precursors) below the mgc, we used static light scattering (SLS) to investigate the extent of self-assembly in the solution of precursors before and after the addition of ALP. As a statistical method to characterize the aggregates, SLS provides the qualitative comparison of aggregates or self-assemblies of precursors in the solution before and after dephosphorylation. All the precursors (**1P**) in the solution exhibit negligible scattering signal (Figure S7), suggesting that there are no detectable assemblies formed by the precursors, even at 500 μM. After the addition of ALP to the solution of **1P**, all of samples exhibit sharp increases of light scattering signals starting at the concentration as low as 200 μM. This result confirms that the dephosphorylation catalyzed by ALP results in the formation of supramolecular assemblies of **1**. Because some hydrogelators (e.g., DDL-1) form large assemblies that precipitate to the bottom of test tube (Figure

S8), it is impossible to correlate the intensity of SLS with the amount of assemblies of the hydrogelators in a quantitative manner.

Despite the existence of the multiscattering issue of hydrogelator assemblies for light scattering, the result from SLS measurements still confirms the formation of supramolecular assemblies of the hydrogelators upon treatment of precursors below mgc (at 500 μM) with ALP. Thus, we used TEM to evaluate the morphology of nanoscale supramolecular assemblies of the hydrogelators (at 500 μM) formed by dephosphorylation. While being consistent with SLS measurement, the TEM images of the precursors at 500 μM (Figure S4) hardly show large amounts of ordered nanostructures, the TEM of the hydrogelators reveals a considerable amount of nanoscale assemblies in different morphologies. For example, upon dephosphorylation catalyzed by ALP, the resulting LLL-1 or DDD-1 self-assembles to form uniform nanofibers with widths of 8 ± 2 nm (Figure 7a,b). The self-assemblies of LLD-1

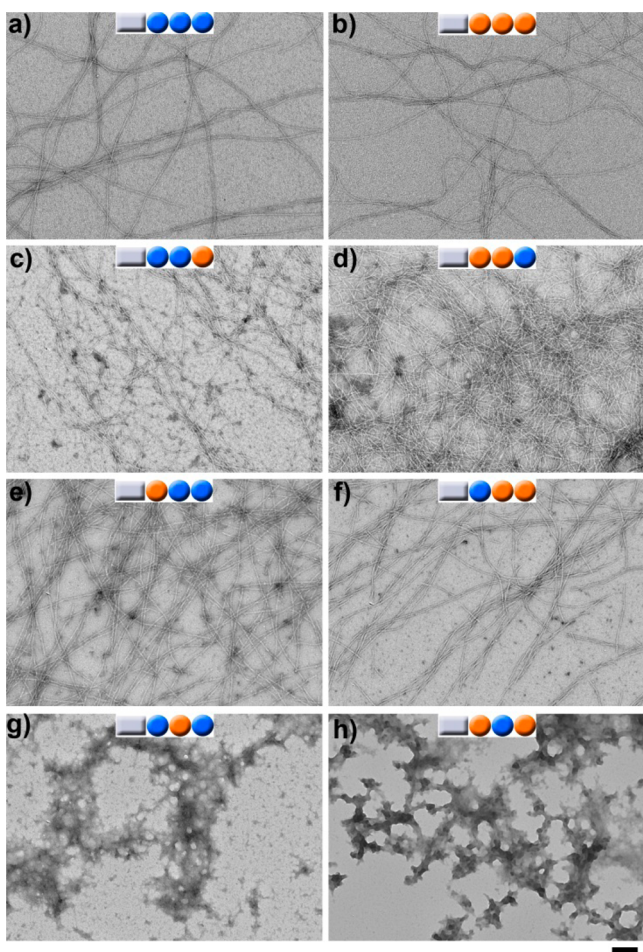


Figure 7. TEM images of the hydrogelators, formed by treating the solution of the precursors (500 μM) with ALP (0.5 U/mL). Scale bar = 100 nm.

and DDL-1 result in uniform nanofibers with widths around 8 ± 2 nm (Figure 7c,d). Some of the nanofibers of DDL-1 exist as bundles, suggesting strong interfiber interactions. The formation of bundles likely causes aggregates to precipitate to the bottom of the test tube (Figure S8). Upon dephosphorylation by ALP, the resulting DLL-1 (or LDD-1) self-assembles to form uniform nanofibers with widths of 9 ± 2 nm (Figure

7e,f). Differing from other isomers, LDL-1 or DLD-1 self-assembles to form disordered and nonfibrillar hydrogelators (formed by ALP after dephosphorylation of precursors (500 μM)), indicating that the supramolecular assemblies of the enantiomeric pairs of the hydrogelators exhibit similar nanoscale morphology (e.g., similar widths of nanofibers), which agrees with the similar cytotoxicities of the enantiomeric pairs of the hydrogelators. It is interesting to note that the morphology at 500 μM is totally different with that at the gel state (0.6 wt %). Since self-assembly is a result of the balance between hydration forces and intermolecular hydrophobic interactions, LDL-1 and DLD-1 interact with more water molecules at low concentration than at high concentration, which likely results in LDL-1 and DLD-1 forming distinct nanostructures at different concentrations. Apparently, the disordered and nonfibrillar nanoscale aggregates of hydrogelators (e.g., the case of LDL-1 and DLD-1) exhibit lower IC_{50} values than those of ordered nanofibers of hydrogelators. This result suggests that the morphology of nanoscale assemblies,⁷⁹ rather than the stereochemistry of individual molecules, determines the cytotoxicity of the supramolecular assemblies of these tripeptidic hydrogelators. This result also agrees with the earlier observation that the morphology of nanoscale assemblies dictates the interaction between proteins and supramolecular assemblies of small molecules.⁸⁷

CONCLUSION

This work examines the cellular response to the enzymatic formation of molecular nanofibers that contain D-amino acid residues. The most noteworthy result is that even though phosphatases (e.g., ALP) quickly convert precursors to the hydrogelators, the precursors exhibit completely different cytotoxicity from those of the hydrogelators due to the location of the endogenous enzymes that convert the precursors to the hydrogelators. Comparing to the use of ligand–receptor interaction, the spatiotemporal control of the formation of molecular nanofibers represents an unprecedented approach to control the fate of cells.⁸⁶ Since the nanofibers formed by the self-assembly of DDD-1 would eventually dissociate to monomeric DDD-1, the cytotoxicity (or other properties) of the nanofibers likely will be transient, which should be a useful feature for designing nanomedicines that function via molecular self-assembly. Therefore, this work may ultimately lead to a new paradigm of supramolecular chemistry. In addition, this work also suggests that judicious incorporation of D-amino acid(s) into peptides is a feasible and useful approach to modulate the morphological and biological properties of supramolecular assemblies of small peptides.^{24,35,45,79,88} Although the detailed mechanism of cytotoxicity of the nanofibers on the cell surface remains to be elucidated, one possible reason for the nanofibers of different conjugates to exhibit different cytotoxicities likely would be that the abilities of the nanofibers to block cell mass exchange with surrounding cells are varied. Furthermore, introducing D-amino acid(s) to supramolecular self-assemblies of peptides^{45,79,89–95} may result in other unexpected biological properties, which is less investigated and warrants further exploration.

ASSOCIATED CONTENT

Supporting Information

Details of the synthesis, NMR spectra, and LC-MS data for all compounds, rheological data, cytotoxicity data, and optical

images. This material is available free of charge via the Internet at <http://pubs.acs.org>.

AUTHOR INFORMATION

Corresponding Author

*E-mail: bxu@brandeis.edu.

Present Address

[†]Key laboratory for Molecular Enzymology and Engineering of the Ministry of Education, Jilin University, 2599 Qianjin St., Changchun 130012, China (Y.H.).

Notes

The authors declare no competing financial interest.

ACKNOWLEDGMENTS

This work was partially supported by NIH (R01CA142746) and Fellowship from Chinese scholar council (2008638092 for J.F.S. and 2010638002 for D.Y.). J.F.S. thanks Mr. R. Haburcak for comments on the manuscript.

REFERENCES

- (1) Hafezi, N.; Lehn, J. M. *J. Am. Chem. Soc.* **2012**, *134* (30), 12861–12868.
- (2) Hirsch, A. K. H.; Buhler, E.; Lehn, J. M. *J. Am. Chem. Soc.* **2012**, *134* (9), 4177–4183.
- (3) Lehn, J. M. *Science* **2002**, *295* (5564), 2400–2403.
- (4) Weisblat, D. A.; Zackson, S. L.; Blair, S. S.; Young, J. D. *Science* **1980**, *209* (4464), 1538–1541.
- (5) Mason, A.; Muller, K. J. *Nature* **1982**, *296* (5858), 655–657.
- (6) Liu, M.; Li, C.; Pazgier, M.; Li, C. Q.; Mao, Y. B.; Lv, Y. F.; Gu, B.; Wei, G.; Yuan, W. R.; Zhan, C. Y.; Lu, W. Y.; Lu, W. Y. *Proc. Natl. Acad. Sci. U.S.A.* **2010**, *107* (32), 14321–14326.
- (7) McDonnell, J. M.; Beavil, A. J.; Mackay, G. A.; Jameson, B. A.; Korngold, R.; Gould, H. J.; Sutton, B. J. *Nat. Struct. Biol.* **1996**, *3* (5), 419–426.
- (8) Merrifield, R. B.; Juvvadi, P.; Andreu, D.; Ubach, J.; Boman, A.; Boman, H. G. *Proc. Natl. Acad. Sci. U.S.A.* **1995**, *92* (8), 3449–3453.
- (9) Eckert, D. M.; Malashkevich, V. N.; Hong, L. H.; Carr, P. A.; Kim, P. S. *Cell* **1999**, *99* (1), 103–115.
- (10) Welch, B. D.; VanDemark, A. P.; Heroux, A.; Hill, C. P.; Kay, M. S. *Proc. Natl. Acad. Sci. U.S.A.* **2007**, *104* (43), 16828–16833.
- (11) Jiang, S. B.; Lu, H.; Liu, S. W.; Zhao, Q.; He, Y. X.; Debnath, A. K. *Antimicrob. Agents Chemother.* **2004**, *48* (11), 4349–4359.
- (12) Suchyna, T. M.; Tape, S. E.; Koeppe, R. E.; Andersen, O. S.; Sachs, F.; Gottlieb, P. A. *Nature* **2004**, *430* (6996), 235–240.
- (13) Pentelute, B. L.; Gates, Z. P.; Dashnau, J. L.; Vanderkooi, J. M.; Kent, S. B. H. *J. Am. Chem. Soc.* **2008**, *130* (30), 9702–9707.
- (14) Morii, T.; Tanaka, T.; Sato, S.; Hagiwara, M.; Aizawa, Y.; Makino, K. *J. Am. Chem. Soc.* **2002**, *124* (2), 180–181.
- (15) Li, J. Y.; Kuang, Y.; Gao, Y.; Du, X. W.; Shi, J. F.; Xu, B. *J. Am. Chem. Soc.* **2013**, *135* (2), 542–545.
- (16) Chalifour, R. J.; McLaughlin, R. W.; Lavoie, L.; Morissette, C.; Tremblay, N.; Boule, M.; Sarazin, P.; Stea, D.; Lacombe, D.; Tremblay, P.; Gervais, F. *J. Biol. Chem.* **2003**, *278* (37), 34874–34881.
- (17) Lupoli, T. J.; Tsukamoto, H.; Doud, E. H.; Wang, T. S. A.; Walker, S.; Kahne, D. *J. Am. Chem. Soc.* **2011**, *133* (28), 10748–10751.
- (18) Ryadnov, M. G.; Degtyareva, O. V.; Kashparov, I. A.; Mitin, Y. V. *Peptides* **2002**, *23* (10), 1869–1871.
- (19) Wei, G. X.; Bobek, L. A. *Antimicrob. Agents Chemother.* **2005**, *49* (6), 2336–2342.
- (20) Lee, D. L.; Hedges, R. S. *Biopolymers* **2003**, *71* (1), 28–48.
- (21) Wakimoto, T.; Mori, T.; Morita, H.; Abe, I. *J. Am. Chem. Soc.* **2011**, *133* (13), 4746–4749.
- (22) Rodriguez-Granillo, A.; Annavarapu, S.; Zhang, L.; Koder, R. L.; Nanda, V. *J. Am. Chem. Soc.* **2011**, *133* (46), 18750–18759.
- (23) Nanda, V.; DeGrado, W. F. *J. Am. Chem. Soc.* **2006**, *128* (3), 809–816.
- (24) Marchesan, S.; Easton, C. D.; Kushkaki, F.; Waddington, L.; Hartley, P. G. *Chem. Commun.* **2012**, *48* (16), 2195–2197.
- (25) Bach, A. C.; Eyermann, C. J.; Gross, J. D.; Bower, M. J.; Harlow, R. L.; Weber, P. C.; Degrado, W. F. *J. Am. Chem. Soc.* **1994**, *116* (8), 3207–3219.
- (26) Krause, E.; Bienert, M.; Schmieder, P.; Wenschuh, H. *J. Am. Chem. Soc.* **2000**, *122* (20), 4865–4870.
- (27) Marchesan, S.; Qu, Y.; Waddington, L. J.; Easton, C. D.; Glattauer, V.; Lithgow, T. J.; McLean, K. M.; Forsythe, J. S.; Hartley, P. G. *Biomaterials* **2013**, *34* (14), 3678–3687.
- (28) Marchesan, S.; Waddington, L.; Easton, C. D.; Kushkaki, F.; McLean, K. M.; Forsythe, J. S.; Hartley, P. G. *BioNanoScience* **2013**, *3* (1), 21–29.
- (29) Rughani, R. V.; Salick, D. A.; Lamm, M. S.; Yucel, T.; Pochan, D. J.; Schneider, J. P. *Biomacromolecules* **2009**, *10* (5), 1295–1304.
- (30) Song, B. B.; Kibler, P.; Malde, A.; Kodukula, K.; Galande, A. K. J. *Am. Chem. Soc.* **2010**, *132* (13), 4508–4509.
- (31) Goto, Y.; Suga, H. *J. Am. Chem. Soc.* **2009**, *131* (14), 5040–5041.
- (32) Fujino, T.; Goto, Y.; Suga, H.; Murakami, H. *J. Am. Chem. Soc.* **2013**, *135* (5), 1830–1837.
- (33) Bong, D. T.; Clark, T. D.; Granja, J. R.; Ghadiri, M. R. *Angew. Chem., Int. Ed.* **2001**, *40* (6), 988–1011.
- (34) Marchesan, S.; Waddington, L.; Easton, C. D.; Winkler, D. A.; Goodall, L.; Forsythe, J.; Hartley, P. G. *Nanoscale* **2012**, *4* (21), 6752–6760.
- (35) Li, Y.; Li, B.; Fu, Y.; Lin, S.; Yang, Y. *Langmuir* **2013**, *29* (31), 9721–9726.
- (36) Schneider, J. P.; Pochan, D. J.; Ozbas, B.; Rajagopal, K.; Pakstis, L.; Kretsinger, J. *J. Am. Chem. Soc.* **2002**, *124* (50), 15030–15037.
- (37) Swanekamp, R. J.; DiMaio, J. T. M.; Bowerman, C. J.; Nilsson, B. L. *J. Am. Chem. Soc.* **2012**, *134* (12), 5556–5559.
- (38) Li, J. Y.; Gao, Y.; Kuang, Y.; Shi, J. F.; Du, X. W.; Zhou, J.; Wang, H. M.; Yang, Z. M.; Xu, B. *J. Am. Chem. Soc.* **2013**, *135* (26), 9907–9914.
- (39) Li, X. M.; Du, X. W.; Li, J. Y.; Gao, Y.; Pan, Y.; Shi, J. F.; Zhou, N.; Xu, B. *Langmuir* **2012**, *28* (37), 13512–13517.
- (40) Liang, G. L.; Yang, Z. M.; Zhang, R. J.; Li, L. H.; Fan, Y. J.; Kuang, Y.; Gao, Y.; Wang, T.; Lu, W. W.; Xu, B. *Langmuir* **2009**, *25* (15), 8419–8422.
- (41) Li, J. Y.; Kuang, Y.; Shi, J. F.; Gao, Y. A.; Zhou, J.; Xu, B. *Beilstein J. Org. Chem.* **2013**, *9*, 908–917.
- (42) Yang, Z.; Liang, G.; Ma, M.; Abbah, A. S.; Lu, W. W.; Xu, B. *Chem. Commun.* **2007**, No. 8, 843–845.
- (43) Yuan, D.; Zhou, R.; Shi, J. F.; Du, X. W.; Li, X. M.; Xu, B. *RSC Adv.* **2014**, *4* (50), 26487–26490.
- (44) Qiu, Z.; Yu, H.; Li, J.; Wang, Y.; Zhang, Y. *Chem. Commun.* **2009**, *23*, 3342–3344.
- (45) Wang, H.; Wang, Y.; Han, A.; Cai, Y.; Xiao, N.; Wang, L.; Ding, D.; Yang, Z. *ACS Appl. Mater. Interfaces* **2014**, *6* (12), 9815–9821.
- (46) Cormier, A. R.; Pang, X. D.; Zimmerman, M. I.; Zhou, H. X.; Paravastu, A. K. *ACS Nano* **2013**, *7* (9), 7562–7572.
- (47) Luo, J. N.; Tong, Y. W. *ACS Nano* **2011**, *5* (10), 7739–7747.
- (48) Rudra, J. S.; Sun, T.; Bird, K. C.; Daniels, M. D.; Gasiorowski, J. Z.; Chong, A. S.; Collier, J. H. *ACS Nano* **2012**, *6* (2), 1557–1564.
- (49) Toft, D. J.; Moyer, T. J.; Standley, S. M.; Ruff, Y.; Ugolkov, A.; Stupp, S. I.; Cryns, V. L. *ACS Nano* **2012**, *6* (9), 7956–7965.
- (50) Lock, L. L.; Cheetham, A. G.; Zhang, P. C.; Cui, H. G. *ACS Nano* **2013**, *7* (6), 4924–4932.
- (51) Laromaine, A.; Koh, L.; Murugesan, M.; Ulijn, R. V.; Stevens, M. M. *J. Am. Chem. Soc.* **2007**, *129* (14), 4156–4157.
- (52) Ulijn, R. V.; Smith, A. M. *Chem. Soc. Rev.* **2008**, *37* (4), 664–675.
- (53) Williams, R. J.; Smith, A. M.; Collins, R.; Hodson, N.; Das, A. K.; Ulijn, R. V. *Nat. Nano* **2009**, *4* (1), 19–24.
- (54) Gao, Y.; Yang, Z.; Kuang, Y.; Ma, M.-L.; Li, J.; Zhao, F.; Xu, B. *Biopolymers* **2010**, *94* (1), 19–31.
- (55) Yang, Z.; Liang, G.; Wang, L.; Xu, B. *J. Am. Chem. Soc.* **2006**, *128* (9), 3038–3043.

- (56) Yang, Z.; Liang, G.; Xu, B. *Acc. Chem. Res.* **2008**, *41* (2), 315–326.
- (57) Bremmer, S. C.; McNeil, A. J.; Soellner, M. B. *Chem. Commun.* **2014**, *50* (14), 1691–1693.
- (58) Toledano, S.; Williams, R. J.; Jayawarna, V.; Ulijn, R. V. *J. Am. Chem. Soc.* **2006**, *128* (4), 1070–1071.
- (59) Zheng, W.; Gao, J.; Song, L.; Chen, C.; Guan, D.; Wang, Z.; Li, Z.; Kong, D.; Yang, Z. *J. Am. Chem. Soc.* **2012**, *135* (1), 266–271.
- (60) Yang, Z. M.; Liang, G. L.; Ma, M. L.; Gao, Y.; Xu, B. *Small* **2007**, *3* (4), 558–562.
- (61) Yang, Z.; Xu, B. *J. Mater. Chem.* **2007**, *17* (23), 2385–2393.
- (62) Sun, Z. F.; Li, Z. Y.; He, Y. H.; Shen, R. J.; Deng, L.; Yang, M. H.; Liang, Y. Z.; Zhang, Y. *J. Am. Chem. Soc.* **2013**, *135* (36), 13379–13386.
- (63) Baral, A.; Roy, S.; Dehsorkhi, A.; Hamley, I. W.; Mohapatra, S.; Ghosh, S.; Banerjee, A. *Langmuir* **2014**, *30* (3), 929–936.
- (64) Babu, S. S.; Praveen, V. K.; Ajayaghosh, A. *Chem. Rev.* **2014**, *114* (4), 1973–2129.
- (65) Majumder, J.; Das, M. R.; Deb, J.; Jana, S. S.; Dastidar, P. *Langmuir* **2013**, *29* (32), 10254–10263.
- (66) Gao, Y.; Berciu, C.; Kuang, Y.; Shi, J. F.; Nicastro, D.; Xu, B. *ACS Nano* **2013**, *7* (10), 9055–9063.
- (67) Chan, W. C.; White, P. D. *Fmoc Solid Phase Peptide Synthesis: A Practical Approach*; Oxford University Press Inc.: New York, 2000.
- (68) Alewood, P. F.; Johns, R. B.; Valerio, R. M.; Kemp, B. E. *Synthesis* **1983**, *1*, 30–31.
- (69) Ottinger, E. A.; Shekels, L. L.; Bernlohr, D. A.; Barany, G. *Biochemistry* **1993**, *32* (16), 4354–4361.
- (70) Shi, J.; Gao, Y.; Yang, Z.; Xu, B. *Beilstein J. Org. Chem.* **2011**, *7*, 167–172.
- (71) Sadeghi-Aliabadi, H.; Minaiyan, M.; Dabestan, A. *Res. Pharm. Sci.* **2010**, *5* (2), 127–33.
- (72) Zhang, Y.; Kuang, Y.; Gao, Y.; Xu, B. *Langmuir* **2010**, *27* (2), 529–537.
- (73) Kuang, Y.; Xu, B. *Angew. Chem., Int. Ed.* **2013**, *52* (27), 6944–6948.
- (74) Saha, S.; Bardelli, A.; Buckhaults, P.; Velculescu, V. E.; Rago, C.; Croix, B. S.; Romans, K. E.; Choti, M. A.; Lengauer, C.; Kinzler, K. W.; Vogelstein, B. *Science* **2001**, *294* (5545), 1343–1346.
- (75) Yang, Z.; Liang, G.; Guo, Z.; Guo, Z.; Xu, B. *Angew. Chem., Int. Ed.* **2007**, *46* (43), 8216–8219.
- (76) Liang, G.; Xu, K.; Li, L.; Wang, L.; Kuang, Y.; Yang, Z.; Xu, B. *Chem. Commun.* **2007**, *40*, 4096–4098.
- (77) Kuang, Y.; Long, M. J. C.; Zhou, J.; Shi, J. F.; Gao, Y.; Xu, C.; Hedstrom, L.; Xu, B. *J. Biol. Chem.* **2014**, DOI: 10.1074/jbc.M114.600288.
- (78) Shi, J.; Pan, Y.; Gao, Y.; Xu, B. *MRS Proc.* **2012**, *1418*, DOI: <http://dx.doi.org/10.1557/proc.2012.331>.
- (79) Marchesan, S.; Easton, C. D.; Styan, K. E.; Waddington, L. J.; Kushkaki, F.; Goodall, L.; McLean, K. M.; Forsythe, J. S.; Hartley, P. G. *Nanoscale* **2014**, *6* (10), 5172–5180.
- (80) Griffin, J. P.; O’Grady, J. *The Textbook of Pharmaceutical Medicine*. Wiley-Blackwell: New York, 2006.
- (81) Giano, M. C.; Pochan, D. J.; Schneider, J. P. *Biomaterials* **2011**, *32* (27), 6471–6477.
- (82) Fishman, W. H.; Inglis, N. R.; Green, S.; Anstiss, C. L.; Gosh, N. K.; Reif, A. E.; Rustigia, R.; Krant, M. J.; Stolbach, L. L. *Nature* **1968**, *219* (5155), 697.
- (83) Yang, Y. L.; Wang, K. T.; Li, W. T.; Adelstein, S. J.; Kassis, A. I. *Chem. Biol. Drug Des.* **2011**, *78* (6), 923–931.
- (84) Chou, J. Y.; Takahashi, S. *Biochemistry* **1987**, *26* (12), 3596–3602.
- (85) Fernley, H. N.; Walker, P. G. *Biochem. J.* **1970**, *116* (3), 543–544.
- (86) Kuang, Y.; Shi, J.; Li, J.; Yuan, D.; Alberti, K. A.; Xu, Q.; Xu, B. *Angew. Chem., Int. Ed.* **2014**, *53* (31), 8104–8107.
- (87) Kuang, Y.; Yuan, D.; Zhang, Y.; Kao, A.; Du, X.; Xu, B. *RSC Adv.* **2013**, *3* (21), 7704–7707.
- (88) Hyland, L. L.; Twomey, J. D.; Vogel, S.; Hsieh, A. H.; Yu, Y. B. *Biomacromolecules* **2012**, *14* (2), 406–412.
- (89) Nagy, K. J.; Giano, M. C.; Jin, A.; Pochan, D. J.; Schneider, J. P. *J. Am. Chem. Soc.* **2011**, *133* (38), 14975–14977.
- (90) Sindhuvanich, C.; Veiga, A. S.; Gupta, K.; Gaspar, D.; Blumenthal, R.; Schneider, J. P. *J. Am. Chem. Soc.* **2012**, *134* (14), 6210–6217.
- (91) Cheetham, A. G.; Zhang, P.; Lin, Y.-a.; Lock, L. L.; Cui, H. *J. Am. Chem. Soc.* **2013**, *135* (8), 2907–2910.
- (92) Shiraki, T.; Morikawa, M.-a.; Kimizuka, N. *Angew. Chem., Int. Ed.* **2008**, *47* (1), 106–108.
- (93) Ariga, K.; Nakanishi, T.; Kawanami, S.-i.; Kosaka, T.; Kikuchi, J.-i. *J. Nanosci. Nanotechnol.* **2006**, *6* (6), 1718–1730.
- (94) Yamamichi, S.; Jinno, Y.; Haraya, N.; Oyoshi, T.; Tomitori, H.; Kashiwagi, K.; Yamanaka, M. *Chem. Commun.* **2011**, *47* (37), 10344–10346.
- (95) Pochan, D. J.; Schneider, J. P.; Kretsinger, J.; Ozbas, B.; Rajagopal, K.; Haines, L. *J. Am. Chem. Soc.* **2003**, *125* (39), 11802–11803.